Amphiphilic polyampholytes for fouling-resistant and easily tunable membranes

Luca Mazzaferro, Samuel J. Lounder, Ayse Asatekin\*

Tufts University, Department of Chemical and Biological Engineering, 4 Colby Street, Medford,

Massachusetts 02155, United States

KEYWORDS: ultrafiltration, nanofiltration, fouling, polyampholyte, self-assembly, membrane

ABSTRACT: The versatility of membranes is limited by the narrow range of material chemistries on the market, which cannot address many relevant separations. Expanding their use requires new membrane materials that can be tuned to address separations by providing the desired selectivity and robustness. Self-assembly is a versatile and scalable approach to create tunable membranes with narrow pore size distribution. This study reports the first examples of a new class of membrane materials that derives state-of-the-art permeability, selectivity, and fouling resistance from the self-assembly of random polyampholyte amphiphilic copolymers. These membranes feature a network of ionic nanodomains that serve as nanochannels for water permeation, framed by hydrophobic nanodomains that preserve their structural integrity. This copolymer design approach enables precise selectivity control. For example, sodium sulfate rejections can be tuned from 5% to 93% with no significant change in pore size or fouling resistance. Membranes developed here have potential applications in wastewater treatment and in chemical separations.

### 1. INTRODUCTION

Chemical separations account for approximately half of the industrial energy consumption in the United States.<sup>1</sup> Compared with other unit operations (*e.g.*, distillation, extraction, chromatography), membranes are excellent candidates for achieving efficient separations: they are scalable, energy efficient, and already widely used in gas and liquid separations.<sup>2</sup> However, their use in many applications is limited by their separation capabilities, fouling resistance, and chemical resistance.<sup>3</sup> Broadening the use of membranes to new separations requires the development of new membrane materials that enable us to tune membrane selectivity to fit increasingly specific separations, while resisting fouling by the feed components.

For example, numerous industrial water recovery and reuse applications require selective removal of organics and divalent ions (*e.g.*, Mg<sup>2+</sup>, SO<sub>4</sub><sup>2-</sup>), while allowing the passage of NaCl.<sup>4-5</sup> Commercially available nanofiltration (NF) membranes have high rejections of these divalent ions, but also exhibit high NaCl retention, which demands higher pressures to overcome osmotic pressure differences and, consequently, incurs higher costs.<sup>6</sup> Moreover, these membranes are highly prone to fouling, quickly losing their permeability when exposed to complex feeds that include biomacromolecules. They are also sensitive to chlorination.<sup>7</sup> As a result, fouling management requires added process steps, leading to increased process complexity, cost, and energy use.<sup>7-8</sup>

Biological separations are particularly challenging applications for membranes. The broad range of specific separations needed in these applications require tunable membranes that can be easily tailored to a given target application.<sup>4,9-10</sup> It is widely accepted that biological drugs, like proteins, peptides, antibody-drug conjugates, and nucleic acids, will play a major role in the future of pharmaceuticals.<sup>11</sup> These active pharmaceutical ingredients present complex molecular structures

with varying sizes and net charges, making efficient separations difficult and costly. Therefore, it is important to develop robust membrane technologies that can keep up with the rapid pace of novel and complex molecules used as clinical therapeutics.<sup>12</sup>

The separation of small organic molecules of similar size but different charges holds great value for several other applications, especially in the extraction and purification of pharmaceutical and nutraceutical compounds such as small molecules, amino acids, peptides, and antibiotics. 13-17 Charged membrane materials with pore walls featuring a fixed net-charge (positive or negative) can achieve this by favoring the passage of solutes that are uncharged or of opposite charge while hindering the passage of co-ions. 18 Traditionally, commercial ultrafiltration (UF) and NF membranes display net-negative charges and broad pore size distributions. These characteristics hinder their usage in numerous applications where highly selective separations are required. While several approaches targeting highly selective separations are being developed, many rely on extremely complex functional materials that lack scalability and ease of manufacture. 19-20

As mentioned previously, membrane fouling is a major challenge that severely limits the broader use of membranes, particularly in applications where feeds have high concentrations of components such as biomacromolecules, particulates, and/or oil. Thus, it is crucial to consider fouling prevention when designing novel membrane materials. Fouling is one of the most relevant fields of study in membrane filtration and is a major obstacle to improving the performance of membrane separation processes.<sup>21</sup> One possible approach to creating high fouling resistance membranes is to mimic zwitterionic chemistries that are already widely accepted as highly fouling resistant.<sup>22-25</sup>

Self-assembly of functional polymeric materials is a powerful tool for designing functional membranes with new capabilities, manufactured through highly scalable processes.<sup>19, 26-28</sup> These

materials often offer enhanced selectivity through the formation of monodisperse, tightly packed pores with pore sizes controlled through polymer chemistry, architecture, and the manufacturing process.<sup>29-30</sup> Self-assembling polymers can also be designed to form controlled surface and pore chemistry. This can lead to highly fouling-resistant membranes.<sup>22-23, 31</sup> These material properties can lead to membranes capable of highly selective separations.<sup>32</sup>

While the literature on the self-assembly of block copolymers is extensive, <sup>19, 33-34</sup> other polymer architectures are needed to access pore sizes <~2 nm. Such small pores are necessary for some particularly interesting separations, including the separation of similarly sized organic compounds and ions. 20, 29-30 Random copolymers of highly incompatible monomers have been shown to form membranes with <2 nm pore sizes. <sup>22-23, 30, 32</sup> Random copolymers are easily polymerized and their fabrication is highly scalable.<sup>35</sup> For example, random zwitterionic amphiphilic copolymers (r-ZACs), which combine a hydrophobic monomer with a zwitterionic monomer, can create bicontinuous structures with great potential in membrane filtration. Most r-ZAC membranes have been shown to have an effective pore size around 1.5 nm, narrow pore size distribution, and excellent fouling resistance.<sup>22-23</sup> The effective pore size can also be decreased by UV cross-linking of specially-designed r-ZACs, leading to membranes with ion selectivity linked to zwitterionic group chemistry. 36-37 Despite these promising features, r-ZACs have some limitations that arise from their chemical structure. First, while various zwitterionic monomers can be synthesized, only a handful are commercially available. Certain charged groups and side groups cannot be feasibly incorporated into a zwitterionic unit due to their bonding structure. Moreover, most zwitterionic monomers exhibit poor solubility in many solvents, further adding to their synthesis challenges. As a result, the range of r-ZAC chemistries that can feasibly be converted to membranes produced at a large scale are limited. Ionic or ionizable monomers, on the other hand, are widely available, cheaper, and typically easier to solubilize.

Polyampholytes, defined as polymers that have anionic and cationic groups in different monomer units, present a relatively unexplored class of hydrophilic polymers. Both zwitterionic and polyampholytic materials have been studied as highly effective chemistries to prevent the adsorption of undesired proteins and other organic macromolecules in part due to their strong hydration shell.<sup>38-40</sup> With only a few instances where polyampholytes were used to enhance fouling resistance on commercial membrane surfaces, 41-42 their application in membrane systems is largely under-studied. Similarly, the self-assembly of amphiphilic polyampholyte copolymers, which contain hydrophobic repeat units in addition to charged repeat units, remains relatively unexplored. Most studies on amphiphilic polyampholytes utilize polyampholyte amphiphilic block copolymers for biomedical applications. 43-44 Some studies show that, in aqueous solutions, amphiphilic polyampholytes can form self-assembled structures such as monolayers, micelles, vesicles, or highly organized structures. 43 The self-assembly behavior of amphiphilic polyampholytes without block architectures, particularly those that are insoluble in water or aqueous media, remains uncharacterized. To the best of our knowledge, this is the first study in which the self-assembly properties of polyampholytes are used in membrane applications, not only enhancing fouling resistance, but also controlling the separation properties of the resulting membranes.

In this paper, we introduce amphiphilic polyampholyte copolymers as new self-assembling materials for membranes with tunable selectivity and exceptional fouling resistance. The membranes developed in this study comprise random Polyampholyte Amphiphilic Copolymers (r-PACs), which combine positively and negatively charged monomer subunits with hydrophobic monomers in a random/statistical copolymer chain, forming a water-insoluble copolymer with

ampholytic chemistry (Figure 1). r-PACs used in this study self-assemble to form a disordered bicontinuous morphology, documented using transmission electron microscopy (TEM). The self-assembled structures and effective pore sizes appear to be influenced by electrostatic interactions between charged side groups along the polymer backbone. Membranes are prepared using a scalable approach, by coating a commercial porous support with a thin layer of r-PAC, resulting in a thin film composite (TFC) membrane. Membrane selectivity can span a broad range of separations, controlled mainly by the anionic to cationic monomer ratio in the copolymer. This material family can be used to form membranes with effective pore sizes varying at least from 1.6 nm to 2.4 nm, sodium sulfate rejections varying from 5 % to 93 %, and remarkable selectivities when separating small organic solutes of similar size but with differing charges. r-PAC TFC membranes also exhibit excellent fouling resistance. The facile tunability and wide range of possible chemical functionalities makes this approach suitable for a variety of applications, in which both fouling resistance and ion selectivity are important factors, including wastewater treatment, biological and ion separations.

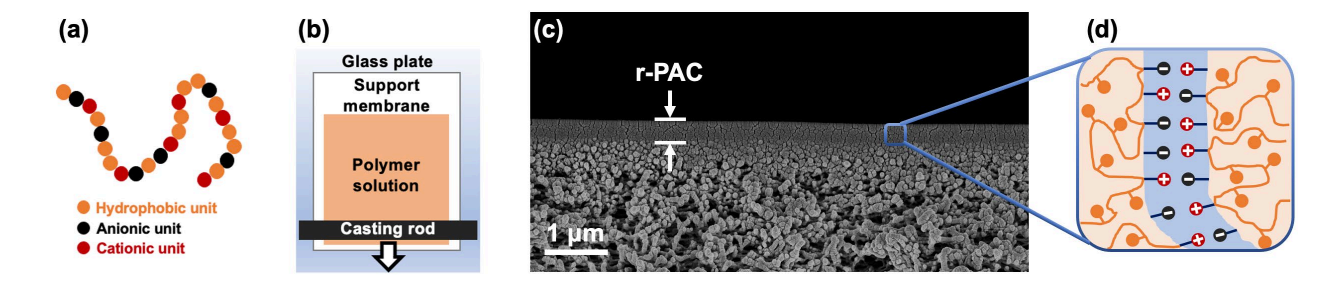


**Figure 1.** Scalable formation of self-assembled r-PAC TFC selective layers. (a) Schematic structure of a random Polyampholyte Amphiphilic Copolymer (r-PAC), with hydrophobic, anionic, and cationic repeat units. (b) Schematic of membrane manufacturing process. A solution of the r-PAC is coated on a commercial porous support membrane (SM). This method is compatible with roll-to-roll manufacturing. (c) Cross-sectional SEM image of a TFC membrane with an r-PAC selective layer on the porous SM. (d) Hypothesized r-PAC self-assembled structure, where ionic domains serve as effective nanopores through which permeation occurs.

## 2. RESULTS AND DISCUSSION

**2.1.** Copolymer Synthesis. We used free radical polymerization (FRP) as a simple and scalable polymer synthesis method to make amphiphilic polyampholytes (Figure 2). To ensure long-term water stability of our membranes, we selected 2,2,2-trifluoroethyl methacrylate (TFEMA) as the hydrophobic monomer for all copolymers in this study. The high hydrophobicity and fluorinated groups of TFEMA make it more likely to phase separate from charged repeat units. Furthermore, our previous studies with amphiphilic copolymers<sup>22-23, 30-31</sup> have shown that TFEMA-containing copolymers are easy to work with due to their better solubility in a wider variety of solvents for casting, likely due to the presence of polar groups in its structure. In this initial study, we selected a polyampholyte ionic pair that mimics a commercially available and well-studied zwitterionic monomer, sulfobetaine methacrylate (SBMA), which is highly hydrophilic and fouling resistant.<sup>22-</sup>

SBMA contains a quaternary amine group connected to a sulfonate group by covalent bonds. Thus, we selected a methacrylate bearing quaternary amine group, [2-(methacryloyloxy)ethyl]trimethylammonium chloride (TAEMA), to form repeat units with a cationic charge throughout a wide pH range. Last, we selected 2-sulfoethyl methacrylate (SEMA) as the anionic monomer, which incorporates an anionic charge when in water over a broad pH range.

**Figure 2.** Synthesis scheme of r-PACs via FRP. (Left) Monomers utilized in this study. (Center) Resulting r-PAC random copolymer structure after FRP. (Right) Resulting r-PAC random copolymer structure after immersion in water.

We synthesized r-PACs with different compositions by altering the molar ratios of the ionic monomers while keeping the mass fraction of the hydrophobic repeat unit constant (Table 1). Three different polyampholyte compositions were selected to demonstrate the tunability of r-PAC membrane materials by small compositional changes. We selected a composition that contains close to a 1:1 molar ratio of anionic and cationic groups, P0. We expected P0 membranes to closely mimic copolymers with charge-neutral zwitterions, exhibiting size-based selectivity along with excellent fouling resistance. The other two compositions exhibit an excess of one of the ionic

monomers, creating a net charge in the membrane layer. P- has an excess of SEMA resulting in a net negative charge, whereas P+ has an excess of the cationic TAEMA. We expect these membranes to have selectivity that is not only size-based but also arising from electrostatic interactions/Donnan exclusion. Additionally, two control polymers were synthesized with only one of the ionic monomers, C- and C+. These polymers are expected to form highly charged selective layers with selectivity arising mostly from electrostatic interactions/Donnan exclusion.

**Table 1.** Monomer composition in the reaction solution and final product for copolymers used in this study.

Copolymer	Reaction solution			Final product			
	lonic units			lonic units			
	SEMA mol%	TAEMA mol%	TFEMA wt%	SEMA mol%	TAEMA mol%	TFEMA wt%	
C-	100	0	50	100	0	60	
P-	70	30	50	65	35	52	
P0	50	50	50	50	50	51	
P+	30	70	50	34	66	51	
C+	0	100	50	0	100	54	

**2.2. Copolymer Characterization.** For all copolymers in this study, <sup>1</sup>H-NMR measurements were used to characterize the chemical composition and calculate the monomer ratios (Table 1, Figure S1-5). Copolymer yields were between 47 % - 66 %. These copolymers would best be described as statistical copolymers, with the monomer sequence determined by the reactivity ratios for each monomer pair. The synthesized copolymers showed a close match between the reaction solution composition and the composition of the resultant copolymer, typically within 5 wt% of each other. This implies that the copolymerization process is likely close to random, with reactivity

ratios close to 1, especially given the fact that copolymer compositions are measured far from full conversion. Therefore, we use the term "random copolymer" throughout the document, though further in-depth characterization of the copolymerization may impart further insight.

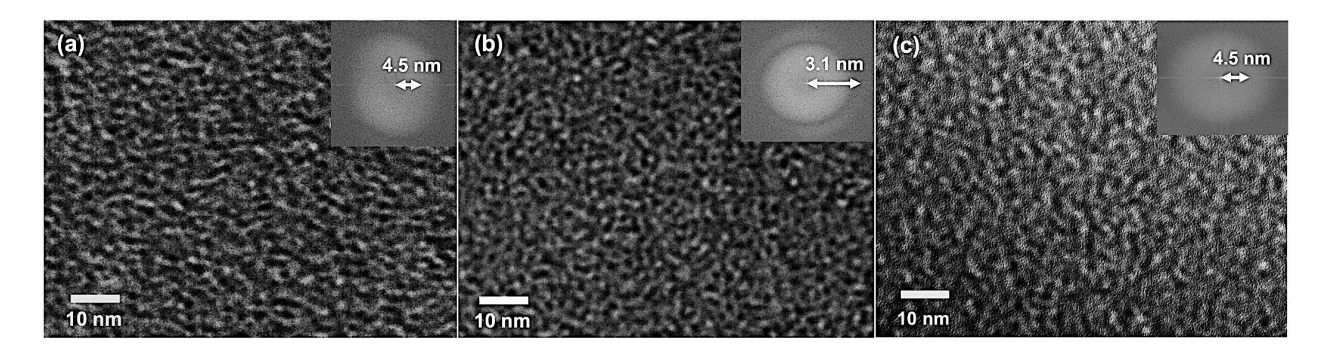
Water uptake measurements are important to understand the degree of swelling of copolymers. 45 We expect that, in r-PACs, water will largely partition into and swell the ionic regions of the polymer. Therefore, the degree of swelling has a direct impact on membrane performance. Water uptake measurements (Table 2) indicate that copolymers with charge ratios closest to 1, and therefore with the highest number of possible polymeric ionic pairs, had the lowest water uptakes, with P0 at 39 % and P-, and P+ at 76 % and 80 %, respectively. Following this trend, the fully negatively and positively charged controls, C- and C+, had the highest water uptakes at 290 % and 970 %, respectively. This can be potentially explained by electrostatics, with P0 having the highest number of possible inter and intra-molecular electrostatic complexes that act as physical cross-links preventing polymer swelling. In contrast, C- and C+ do not exhibit polymer-polymer electrostatic attraction but instead electrostatic repulsive interactions between polymer chains in water. Consequently, C- and C+ showed the highest water uptakes and a hydrogel-like behavior.

Table 2. Polymer yield, glass transition, and water uptake of copolymers used in this study.

	C-	P-	Р0	P+	C+
Polymer yield (%)	55	58	47	66	46
T <sub>g</sub> (°C)	92	137	168	160	156
Water uptake (%)	288 ± 14	76 ± 4	39 ± 3	80 ± 4	971 ± 78

## 2.3. Copolymer Self-Assembly Characterization.

We used TEM to characterize the self-assembled morphology of our r-PACs. The ionic domains were positively stained by immersion in 2 % aqueous CuCl<sub>2</sub> solution. We expect the copper ions to only go into the water-permeable ionic/ampholytic domains. Staining is further supported by the formation of sulfonate-copper complexes. 46 Figure 3 shows brightfield TEM images of P-, P0, and P+ copolymers. All images show a disordered bicontinuous morphology, with a network of percolated ionic nanochannels (dark regions) surrounded by the hydrophobic phase (light regions). This morphology is consistent with previously reported random copolymers with highly incompatible repeat units, including r-ZACs.<sup>23, 37</sup> The fast Fourier transform (FFT) of the TEM image lacked directional features (insets in Figure 3), indicating an isotropic structure, as expected.<sup>23, 37</sup> The characteristic length scale given by the outer ring of the FFT was 4.5 nm, 3.1 nm, and 4.5 nm for P-, P0, and P+ respectively, corresponding to a dry state average ionic domain size of approximately 2.2 nm, 1.5 nm, and 2.2 nm for P-, P0, and P+, respectively. These results indicate that P- and P+ have similar ionic domain sizes in dry state, while P0 was the smallest ionic domain size. In water, the ionic domains will likely swell somewhat. However, these water "channels" are partially occupied by the ionic polymer backbone and side groups. Therefore, the space, or pore size, available for solute permeation would be smaller than the swollen domain size. Therefore, we expect these domain sizes to be closely correlated with the effective pore sizes of membranes manufactured from each polymer.



**Figure 3.** TEM bright-field images of r-PAC self-assembled morphologies with different -/+ charge ratio but similar hydrophobic monomer content, showing bicontinuous networks of ionic nanochannels (dark) surrounded by the hydrophobic phase (light). (Inset) FFT of the image with the arrow corresponding to the characteristic period of both ionic and hydrophobic domains. (a) P- exhibits a characteristic period of ~4.5 nm, yielding a dry ionic channel size around 2.2 nm. (b) P0 exhibits a characteristic period of ~3.1 nm, yielding a dry ionic channel size around 1.5 nm. (c) P+ exhibits a characteristic period of ~4.5 nm, yielding a dry ionic channel size around 2.2 nm.

To further characterize phase separation, we utilized differential scanning calorimetry (DSC), where different glass transition temperatures can be related to different phases or domains. 47-48 When studying a copolymer with only two distinct monomer units, a fully phase separated copolymer is expected to exhibit two distinct T<sub>g</sub>s, each corresponding to one domain. 47-48 A copolymer whose repeat units form a single phase exhibits a T<sub>g</sub> that follows the Fox Equation, particularly if there are no specific interactions between different types of repeat units. 49 For copolymers with interacting groups, analysis may be more complex. For instance, in a polymer with multiple distinct monomeric units, it is possible for two monomeric components to segregate into the same phase, and interactions between repeat units may change chain mobility and hence

the T<sub>g</sub> of a given phase.<sup>50</sup> It is also challenging to characterize the phase separation behavior of a copolymer when one of the  $T_{\rm g}s$  is unknown and above degradation temperature, as is the case for SEMA. Nonetheless, thermal analysis can give insights into the self-assembly of these copolymers. DSC analysis showed a single glass transition for all copolymers in this study (Table 2). Only C- showed a glass transition at temperatures around the homopolymer T<sub>g</sub> of PTFEMA (~84 °C). This suggests that C- is a copolymer with a fully phase separated structure, similar to Nafion.<sup>47</sup> It is likely that the Tg corresponding to the SEMA phase is higher than the degradation temperature (Figure S7). The T<sub>g</sub> observed for the C+ is much higher than the expected mixed phase T<sub>g</sub> values predicted by the Fox equation for this copolymer composition but slightly lower than the Tg of TAEMA homopolymers. This indicates that the observed T<sub>g</sub> for C+ likely corresponds to a phase that is richer in TAEMA monomer units than the single phase predicted by the Fox Equation, thus implying a separate, PTFEMA-rich phase. The TAEMA rich phase contains some TFEMA segments that plasticize it, likely due to the fact that the repeat units cannot separate completely due to the random sequence of repeat units along the copolymer backbone. The Tg of the TFEMArich phase is not observed. This has been previously reported for microphase-separated random copolymers and arises from the fact that the short PTFEMA segment size in these domains cannot acquire mobility until the more rigid, high Tg phase becomes mobile.23,51 P-, P0, and P+ also behave similarly, implying they have similar phase separated structures, particularly in light of the TEM analysis also indicating phase separation. Further in-depth thermal characterization of r-PAC

**2.4. Membrane Formation.** All TFC membranes were prepared by coating a 5 wt% copolymer solution on top of a commercial polysulfone ultrafiltration membrane (PS35, Solecta) using a wirewound metering rod (Gardco, #8). When casting P-, P0, P+, and their respective controls, C- and

polymers may reveal further insight.

C+, we utilized 2,2,2-trifluoroethanol (TFE) as the casting solvent and a 30s solvent evaporation time prior to precipitating the copolymer in DI water as the non-solvent.

As seen in Figure 4, all copolymers except for C+ formed a visible and dense selective layer on top of the support membrane, with thicknesses varying between 300-500 nm. Most commercial ultrafiltration membranes have a mild net negative charge in water,<sup>52</sup> a common practice in the membrane industry to delay and limit fouling by the most common foulants in water and wastewater treatment (e.g., humic acid, alginate, bacteria). The presence of a net anionic surface charge was documented for the PS35 support membrane by filtering small solutes containing different net charges (Table S8). Anionic small organic molecules much smaller than the nominal molecular cut-off (MWCO) of this membrane, 20 kDa, were rejected by up to 51 % while similarly sized neutral solutes had rejections <6 %. This behavior is consistent with a net negative surface charge, leading to the exclusion of charged solutes from the pores. It is likely that this negative charge, in combination with capillary forces, drove the highly positively charged copolymer C+ into the support porous network, preventing the formation of a well-defined selective layer for that control. This was likely facilitated by the fact that the hydrodynamic diameter of C+, measured by dynamic light scattering (DLS) to be ~8.5 nm (Table S9), was smaller than the pore size corresponding to the nominal MWCO of the SM (~9 nm, which corresponds to the hydrodynamic diameter of poly(ethylene oxide) with a molecular weight of 20 kDa).<sup>53</sup>

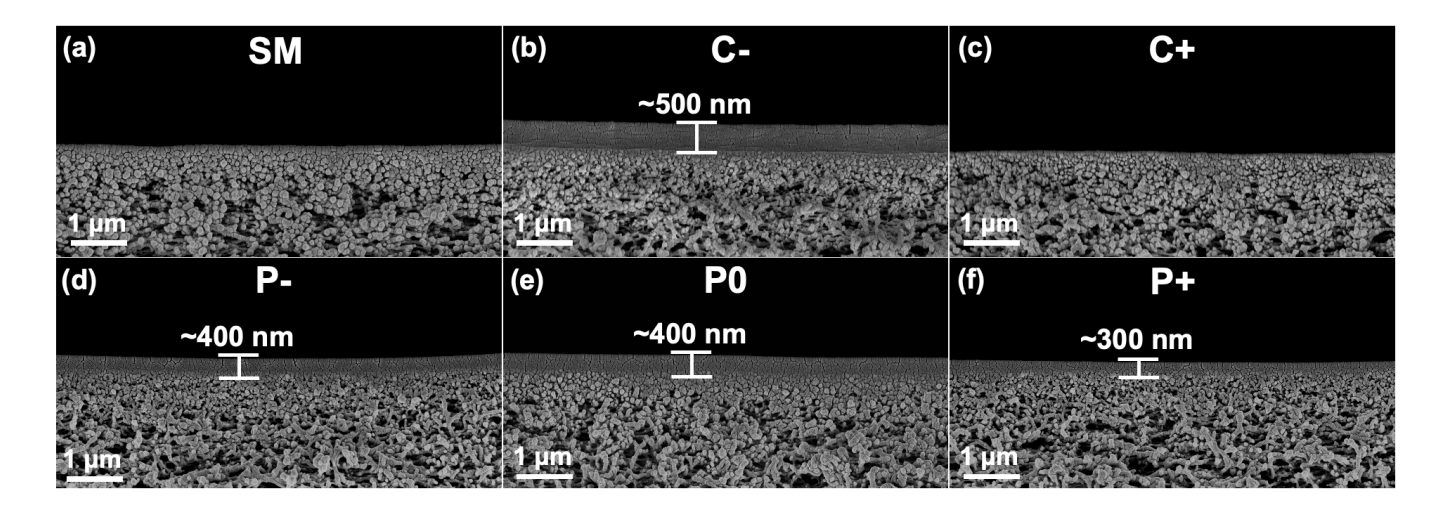


**Figure 4.** Cross-sectional FESEM images of uncoated support membrane and TFC membranes with selective layers made of amphiphilic ionic copolymers. (a) Uncoated support membrane (SM), (b) C-, (c) C+, (d) P-, (e) P0, and (f) P+. All, except for C+ show a dense ~300-500 nm copolymer coating as indicated by arrows (100 000× magnification).

## 2.5. Membrane Performance.

To characterize the membrane performance, we performed dead-end stirred cell filtration experiments testing three distinct membrane disks for each copolymer. To evaluate the effective pore sizes of our membranes we filtered a series of neutral organic solutes with known Stokes radii (glycerol, glucose, sucrose, vitamin B12, and myoglobin, Table S2) (Figure 5). The rejection data for each membrane was fitted to the Donnan Steric Pore Model with a single pore diameter to calculate the effective pore size.<sup>37</sup>

The charge-balanced r-PAC TFC membrane, P0, had a permeance of 2 L/m².h.bar and an effective pore size of 1.6 nm (Table 3). The charged polyampholytes, P- and P+, had higher permeances, 5 and 10 L/m².h.bar, respectively. Interestingly, P- and P+ had identical effective pore sizes, both at 2.4 nm (Table 3). We expect these permeances can be further improved through better coating procedures that decrease layer thickness.<sup>31</sup> These effective pore sizes are similar to

domain sizes observed in TEM imaging, further supporting the transport of solutes through the ampholytic nanodomains. These results demonstrate the facile pore size tunability of these membranes by leveraging the copolymer composition. It is conceivable that other monomer ratios can be explored to access a continuum of available effective pore sizes. The controls, C- and C+ showed much higher permeances, both above 100 L/m².h.bar. These results are consistent with the much higher water uptake of these controls compared with polyampholyte copolymers (Table 2), as well as the much lower rejection of tested solutes, implying a large effective pore size.

**Table 3.** Pure water permeance, and effective pore size of copolymers used in this study.

	C-	P-	PO	P+	C+
Permeance (L/(m².h.bar))	108 ± 10	5 ± 1	2 ± 0.5	10 ± 1.5	112 ± 12
Effective pore size (nm)	16	2.4	1.6	2.4	22

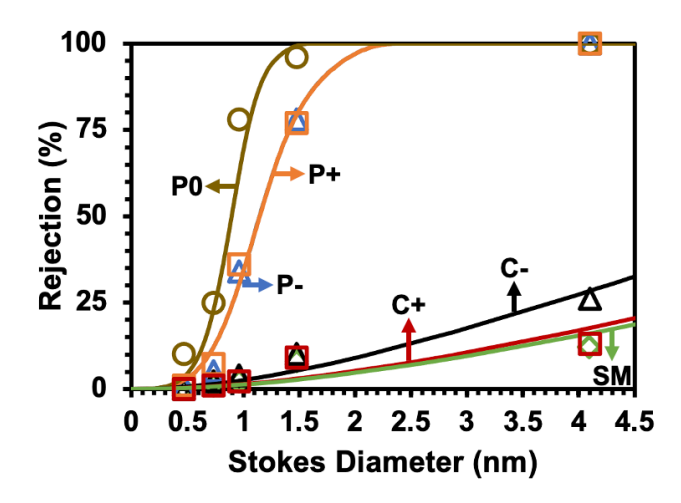


**Figure 5.** Rejection of neutral solutes vs Stokes diameter for uncoated SM and TFC membranes with selective layers made of amphiphilic ionic copolymers. Solid lines are fits to the DSPM<sup>37, 54</sup> for uniform effective pore diameters (Table 3).

Past studies on polyampholyte and polyelectrolyte hydrogels have shown that the swelling behavior of these two polymer classes is strongly affected by the ionic strength of the solution and electrostatic interactions between polymer chains. 55-57 Polyelectrolyte and polyampholyte hydrogels with strong charge imbalance have exhibited a polyelectrolyte effect, the hydrogel decreases swelling with increasing ionic strength solutions. 55-57 Neutral polyampholyte hydrogels have shown the opposite behavior, increased swelling with increasing ionic strength solutions, also known as the antipolyelectrolyte effect. 55-57 All copolymers in this study showed no change in permeance or swelling when using salt concentrations up to 10 mM. This is likely due to the hydrophobic component of the copolymer that arrests the structure, preventing the swelling or deswelling of the copolymers. The degree of swelling and permeance of these membranes appears to be determined by the amount of attractive (polyampholyte) and repulsive (polyelectrolyte) interactions between polymer chains. Thus, by controlling the copolymer composition, r-PACs

can effectively manipulate the balance between attractive and repulsive Coulombic interactions, enabling easy tuning of membrane performance.

Charged membrane materials in which pore walls feature a fixed net charge (positive or negative) can achieve the separation of similar sized solutes by favoring the passage of solutes that are uncharged or of opposite charge but hindering the passage of co-ions. <sup>18</sup> To evaluate the charge-based selectivity between organic solutes we selected four dyes with varying electrostatic charges and similar sizes (~1 nm) (Figure 6): Ethyl Orange (anionic, -1), Acid Blue 45 (anionic, -2), Riboflavin (neutral), and Pararosaniline (cationic, +1). In the proposed membranes, electrostatic interactions between the solutes and the net charged pore walls of P- and P+ are expected to play a dominant role on solute permeation. Thus, solute rejection is expected to strongly depend on solute charge, leading to charge-based separation capabilities. <sup>30</sup> In the case of P0, steric effects are expected to dominate over electrostatic interactions due to the expected net neutral pore walls.

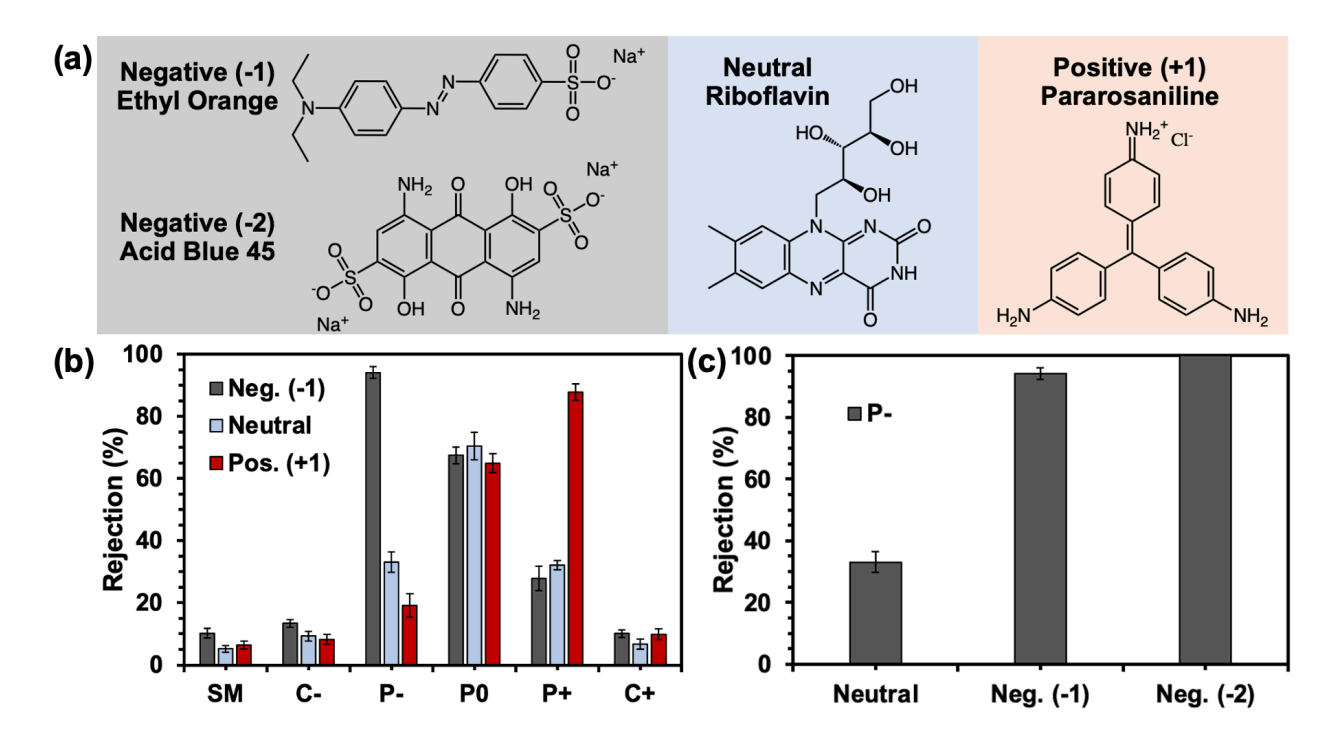


**Figure 6.** (a) Chemical structures and charges of dyes used in this experiment. (b) Rejection of single dye solutes with varying charge (Negative: Ethyl Orange, Neutral: Riboflavin, Positive: Pararosaniline) for uncoated SM and for TFC membranes with selective layers made of amphiphilic ionic copolymers. (c) Rejection of single dye solutes with varying charge for P-membrane (Neutral: Riboflavin, Neg. (-1): Ethyl Orange, Neg. (-2): Acid Blue 45).

Figure 6 shows the rejection of organic solutes with varying electrostatic charges and similar sizes by all TFC membranes developed in this study. P0 shows very similar retention of the three solutes with different charges, indicative of a net neutral membrane that exhibits size-based separation. P- shows a much higher rejection of the negatively charged Ethyl Orange at 94 % when compared to only 19 % rejection of the positively charged Pararosaniline. In a similar manner, P-rejects 100 % of doubly negatively charged solute Acid Blue 45. These results show how r-PAC membranes are good candidates for the treatment of paint industry wastewater, where highly toxic,

charged azo dyes are present.<sup>58</sup> Much lower rejections are observed for neutral and cationic dyes for P-. The support (SM), C-, and C+ all exhibited low rejections (<15 %) for all dyes, consistent with their large effective pore sizes. These results demonstrate that r-PAC membranes are not only strong candidates for application where charge-based selectivity for either charge (positive or negative) is required but also if a net neutral membrane is desired.

To better understand the charge-based selectivity of these membranes and their potential for water softening applications and other ion-based separations, we measured the rejections of two divalent salts, MgCl<sub>2</sub> and Na<sub>2</sub>SO<sub>4</sub> (Figure 7). Donnan model predicts that a homogeneous and anionically charged selective layer would exhibit higher rejection of salts of doubly charged anions (e.g., Na<sub>2</sub>SO<sub>4</sub>) than those of doubly charged cations (e.g., MgCl<sub>2</sub>). In contrast, a cationically charged layer would display the opposite rejection behavior, rejecting MgCl<sub>2</sub> more than Na<sub>2</sub>SO<sub>4</sub>. <sup>54</sup>, <sup>59-61</sup> As it is widely established by the Donnan exclusion mechanism, when the ionic strength of a solution increases charge screening effects will increase as well. <sup>61</sup> Therefore, we should expect a lower rejection of salts at higher salt concentrations when using charged selective layers. In contrast, we expect no change in rejection at different salt concentrations when using net neutral selective layers.

The charge-balanced P0 membrane exhibited Na<sub>2</sub>SO<sub>4</sub> rejections around 76 % and MgCl<sub>2</sub> rejections around 31 % (Figure 7). There was no significant change in rejection with ionic strength, in agreement with the overall net neutral charge of this selective layer. In contrast, membranes with net charge showed significant decreases in rejection with ionic strength. P- exhibited high Na<sub>2</sub>SO<sub>4</sub> rejection (96 % - 93 %), in agreement with the net anionic charge of the membrane as well as its nano-scale pores, similar to many NF membranes. Its MgCl<sub>2</sub> rejection, in contrast, is much lower, below 20 %. The P+ membrane, in agreement with its net charge, had much higher MgCl<sub>2</sub>

rejection than Na<sub>2</sub>SO<sub>4</sub>, with both values decreasing with ionic strength. The behavior of the C- and C+ membranes are also in agreement with a selective layer with higher charge density, yet larger pores, consistent with Donnan exclusion mechanisms. Their salt rejections were lower, and much more sensitive to ionic strength as they relied more heavily on Donnan exclusion. Although not visible in the SEM image (Figure 4), C+ clearly performs as a cationic membrane (Figure 7), confirming the presence of the coating on the support.

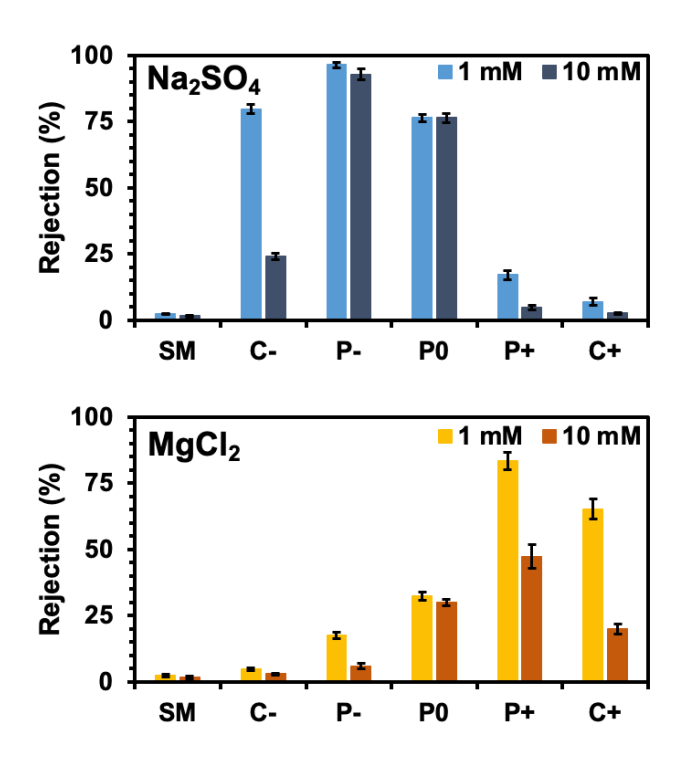


**Figure 7.** Rejection of single salts at different salt molar concentrations for uncoated SM and TFC membranes with selective layers made of amphiphilic ionic copolymers.

Fouling is a major obstacle to the efficiency, operability, and even technical feasibility of membrane separation processes.<sup>21</sup> Membranes that exhibit minimal fouling have been shown to enable cost savings up to 46 % compared with standard systems.<sup>62</sup> Additionally, membrane fouling

severely limits the broader use of membranes in applications where feeds have high concentrations of components such as biomacromolecules, particulates, and/or oil. Therefore, it is crucial to consider fouling prevention in designing novel membrane materials. Previous studies have shown that polyampholytic surface coatings and hydrogels can exhibit excellent fouling resistance<sup>41-42, 63-64</sup>, particularly if they are charge-balanced and net neutral. However, the effect of incorporating mismatched charges or hydrophobic comonomers is not yet studied in a thin film composite membrane.

To screen the fouling resistance of our newly-developed r-PACs, 25-hour fouling experiments were performed in a dead-end stirred cell system. While this system is not representative of most industrial systems, it is a "stress test" for membranes as the feed concentration increases throughout the experiment. For this study, we selected a major membrane foulant, oil. Large volumes of oily wastewaters are produced by manufacturing, oil, and petroleum industries and their adequate disposal or treatment remains a big challenge. 65-66 The representative fouling solution was 1500 ppm oil-in-water emulsion prepared using 9:1 ratio of soybean oil to DC193 surfactant formulated to mimic oily wastewater streams. <sup>66</sup> After 25 hours of filtering this solution, the membranes were rinsed with deionized water to simulate a physical cleaning, and pure water permeance was measured once again. All three r-PAC membranes, P-, P0, and P+ showed excellent fouling resistance demonstrated by minimal flux decline during the fouling test and after water rinse. In contrast, the commercial PES membrane irreversibly lost about half of its initial flux (Figure 8), consistent with previous studies using various commercial membranes.<sup>67-69</sup> This demonstrates that self-assembled polyampholytes are highly promising materials to create fouling resistant and easily tunable membranes. A possible application of r-PAC membranes is the treatment of food industry wastewater, 70 where the retention of oils, proteins, and other biological

components can create value on the permeate side by removing contaminants but also on the feed side by creating organic feedstock. We expect to conduct a deeper study on the fouling resistance properties and mechanisms in this new material family as a next step.

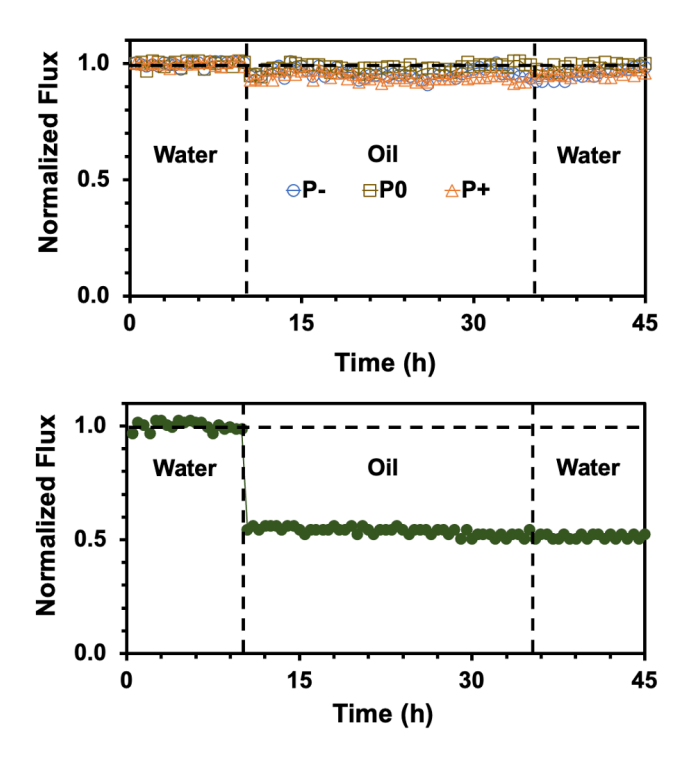


**Figure 8.** Dead-end filtration of oil-in-water emulsions through TFC membranes with selective layers made of (Top) P-, P0, and P+, (Bottom) commercial nanofiltration membrane of similar pore size (NP030). P-, P0, and P+ membranes showed negligible decline in water flux after oil-in-water emulsion filtration. The commercial membrane showed 50 % irreversible flux loss. Horizontal and vertical dotted lines are for visual aid.

# 3. CONCLUSIONS

This is, to our knowledge, the first time polyampholyte amphiphilic copolymers were used as membrane selective layers. This new class of TFC layer derives its membrane performance from

polymer self-assembly. Our results demonstrate a close correlation between the self-assembled nanostructure of the copolymer, and the performance of membranes whose selective layers they form. Furthermore, the self-assembled domain size of r-PACs, and thus the effective pore size of resultant membranes, can be easily tuned by altering the anionic to cationic repeat unit ratios. Depending on polymer composition the membranes can selectively reject solutes of either charge (negative or positive) or rely solely on size-based selectivity as the anionic to cationic repeat unit ratio is 1 (neutral layer). These membranes exhibit commercially viable pure water permeabilities. They are also resistant to irreversible fouling, showing negligible flux decline upon filtering an oil-in-water emulsion. The tunable selectivity, exceptional fouling resistance, and ease of fabrication of these membranes makes them promising for biomolecule separations, textile wastewater treatment, filtration of feeds with large fouling potential, and feeds where charge-based selectivities are desired. It is important to note that this work only entails one combination of ionic monomers, we foresee that the exploration of different monomer combinations can produce r-PACs with different membrane performances and a variety of additional applications.

#### 4. EXPERIMENTAL SECTION

**4.1. Copolymer Synthesis.** TAEMA and SEMA were passed through a column of neutral activated alumina to remove inhibitors, while the TFEMA was passed through a column of basic activated alumina.

Synthesis of P0 (P(TFEMA-r-TAEMA-r-SEMA)). SEMA (2.42 g, 12.4 mmol), TAEMA (2.58 g, 12.4 mmol), and TFEMA (5.00 g, 29.7 mmol) were dissolved in this order in dimethyl sulfoxide (DMSO, 40 mL). Azobisisobutyronitrile (AIBN, 0.01 g) was added to the flask. The flask was sealed, and nitrogen was bubbled through the reaction mixture for 30 minutes to purge any

dissolved oxygen. The flask was then placed in an oil bath set to 60 °C, while stirring at 300 rpm for 17 hours. The flask was removed from the oil bath and unsealed, and 1 g of 4-methoxyphenol (MEHQ) was added to terminate the reaction. The reaction mixture was then precipitated in acetone (1 L), purified by stirring two fresh portions of 1:5 methanol to acetone volume ratio for at least 5 hours, and two fresh portions of acetone for at least 5 hours. Finally, the copolymer was dried in the vacuum oven for 72 hours at 60 °C. The yield was about 45 %.

Synthesis of P- (P(TFEMA-r-TAEMA-r-SEMA)). SEMA (3.39 g, 17.5 mmol), TAEMA (1.55 g, 7.5 mmol), and TFEMA (4.94 g, 29.4 mmol) were dissolved in this order in DMSO (40 mL). AIBN (0.01 g) was added to the flask. The flask was sealed, and nitrogen was bubbled through the reaction mixture for 30 minutes to purge any dissolved oxygen. The flask was then placed in an oil bath set to 60 °C, while stirring at 300 rpm for 17 hours. The flask was removed from the oil bath and unsealed, and 1 g of MEHQ was added to terminate the reaction. The reaction mixture was then precipitated in 1:1 acetone to hexane volume ratio (1 L), purified by stirring two fresh portions of 1:3 ethanol to hexane volume ratio for at least 5 hours, and two fresh portions of acetone for at least 5 hours. Finally, the copolymer was dried in the vacuum oven for 72 hours at 60 °C. The yield was about 58 %.

Synthesis of P+ (P(TFEMA-r-TAEMA-r-SEMA)). SEMA (1.45 g, 7.5 mmol), TAEMA (3.61 g, 17.4 mmol), and TFEMA (5.06 g, 30.1 mmol) were dissolved in this order in DMSO (40 mL). AIBN (0.01 g) was added to the flask. The flask was sealed, and nitrogen was bubbled through the reaction mixture for 30 minutes to purge any dissolved oxygen. The flask was then placed in an oil bath set to 60 °C, while stirring at 300 rpm for 17 hours. The flask was removed from the oil bath and unsealed, and 1 g of MEHQ was added to terminate the reaction. The reaction mixture was then precipitated in acetone (1 L) and purified by stirring two fresh portions of 1:3 ethanol to

hexane volume ratio for at least 8 hours. Finally, the copolymer was dried in the vacuum oven for 72 hours at 60 °C. The yield was about 66 %.

Synthesis of C- (P(TFEMA-r-SEMA)). SEMA (4.00 g, 20.6 mmol), and TFEMA (4.00 g, 23.8 mmol) were dissolved in this order in DMSO (32 mL). AIBN (0.008 g) was added to the flask. The flask was sealed, and nitrogen was bubbled through the reaction mixture for 30 minutes to purge any dissolved oxygen. The flask was then placed in an oil bath set to 60 °C, while stirring at 300 rpm for 17 hours. The flask was removed from the oil bath and unsealed, and 0.8 g of MEHQ was added to terminate the reaction. The reaction mixture was then precipitated in 1:3 ethanol to hexane volume ratio (0.8 L) and purified by stirring two fresh portions of 2:3 ethanol to hexane volume ratio for at least 3 hours. Finally, the copolymer was dried in the vacuum oven for 72 hours at 60 °C. The yield was about 55 %.

Synthesis of C+ (P(TFEMA-r-TAEMA)). TAEMA (4.00 g, 19.3 mmol), and TFEMA (4.00 g, 23.8 mmol) were dissolved in this order in DMSO (32 mL). AIBN (0.008 g) was added to the flask. The flask was sealed, and nitrogen was bubbled through the reaction mixture for 30 minutes to purge any dissolved oxygen. The flask was then placed in an oil bath set to 60 °C, while stirring at 300 rpm for 17 hours. The flask was removed from the oil bath and unsealed, and 0.8 g of MEHQ was added to terminate the reaction. The reaction mixture was then precipitated in acetone (0.8 L) and purified by stirring two fresh portions of 1:3 ethanol to hexane volume ratio for at least 3 hours. Finally, the copolymer was dried in the vacuum oven for 72 hours at 60 °C. The yield was about 45 %.

**4.2.** Copolymer Characterization. The synthesized copolymers were characterized using <sup>1</sup>H nuclear magnetic resonance (<sup>1</sup>H NMR) spectroscopy. After dissolving the copolymers in DMSO-

d<sub>6</sub>, NMR spectra were acquired on a Bruker AVANCE III 500 MHz spectrometer. All samples were scanned 32 times using a 10 s relaxation delay.

TEM was performed using a Hitachi 7800 transmission electron microscope operated in bright-field mode at 100 keV. Copolymer films were prepared by evaporating the solvent from a 5 wt% copolymer/TFE solution in a Teflon dish. Ionic domains were stained by immersing the films in a 2 wt% solution of CuCl<sub>2</sub> for 4 h. The stained films were then embedded in an epoxy resin, sectioned to 50 nm using an ultramicrotome, and transferred to copper grids. The imaging was performed by Dr. Nicki Watson at the Harvard Center for Nanoscale Systems (CNS). TEM images were analyzed using ImageJ software.

DSC was performed utilizing a TA Q100 series calorimeter (TA Instruments) coupled with a  $N_2$  purge and cooling systems. 4-5 mg of each polymer was sealed in aluminum pans, and fully dried under  $N_2$  in the DSC chamber to avoid  $T_g$  shifts due to different water contents. After samples were fully dried, a modulated heating ramp of 5 °C/min was used. The  $T_g$  of all samples was obtained from the midpoint of the baseline shift.

ATR-FTIR spectroscopy was performed using an FT/IR-6200 spectrophotometer (JASCO Corp) equipped with a ZnSe crystal. ATR-FTIR spectra (4000–600 cm<sup>-1</sup>, 4 cm<sup>-1</sup> resolution, 64 scans) were collected using films prepared by drying a 5 wt% solution of polymer in TFE on a Teflon dish. Water uptake measurements were performed by utilizing the same polymer films used for ATR-FTIR analyses. First the films were equilibrated in deionized water at room temperature overnight. Excess water was removed by placing the films onto a Kimwipe for 5 s, after that the samples were weighted. The dry weight was obtained from drying the same samples overnight in a vacuum oven set at 60 °C.

**4.3. Membrane Fabrication and Characterization.** Membranes were prepared using 5 wt% solutions of polymer dissolved in TFE. All polymer solutions were passed through a 0.45 micrometer syringe filter (Whatman) and degassed in a vacuum oven for at least 1 h. The membranes were prepared by coating a thin layer of polymer solution on a commercial ultrafiltration (UF) membrane using a wire-wound metering rod (Gardco, #8). PS35 ultrafiltration membrane (nominal MWCO 20 kDa), purchased from Solecta (Oceanside, Calif.), was used as received as the support membrane. 30 s after coating, the membrane was immersed in a deionized water bath. Membranes were stored in deionized water for several hours before usage.

The thin film composite layers were characterized by a FESEM Ultra Plus (Carl Zeiss, Inc.) using 5 kV and 4.6 mm working distance. Dried membranes were immersed in liquid nitrogen and severed with a razor blade for cross-sectional imaging. Samples were sputter coated (Cressington 108 manual, Ted Pella Inc., CA) with Au/Pd (60/40) in argon atmosphere.

**4.4. Filtration Experiments.** Water fluxes and solute rejections were measured using 10 mL Amicon 8010 dead-end stirred cells (Millipore) with filtration area of 4.1 cm<sup>2</sup>, stirred at 500 rpm, at a trans-membrane pressure of 40 psi. Flux was calculated by monitoring the mass of permeate, collected on a scale (Ohaus Scout Pro) connected to a computer. Permeance is a membrane property that normalizes the flux to account for the trans-membrane pressure, and is calculated using

$$L_p = \frac{J}{\Delta p} \tag{1}$$

where  $L_p$  is the permeance of the membrane (L m<sup>-2</sup> h<sup>-1</sup> bar<sup>-1</sup>), J is the water flux across the membrane (L m<sup>-2</sup> h<sup>-1</sup>), and  $\Delta p$  is the trans-membrane pressure (bar).

The effective pore size of each membrane was determined by filtering a series of organic solutes (sugars and dyes), sugars at a 4000 ppm concentration, and dyes at a 0.1 mM concentration. Salt

and charge-based selectivity was determined by filtering salts at two different concentrations, 1 mM and 10 mM. For all rejection tests the first milliliter of filtrate was discarded, and the subsequent 1 mL was collected and used for measuring rejection. This procedure was previously determined to be appropriate for acquiring steady rejection values.<sup>31</sup> Solute concentration was measured using a conductivity meter (high range, VWR), COD kits (K-7365, CHEMetrics), or a UV–vis spectrometer (Genesys10, ThermoScientific). Rejection was calculated using

$$R(\%) = \frac{(c_f - c_p)}{c_f} \times 100\% \tag{2}$$

where R is the solute rejection (%),  $C_f$  is the feed concentration (mg/L), and  $C_p$  is the permeate concentration (mg/L).

For the fouling experiments, a feed solution consisting of 1500 ppm oil-in-water emulsion (9:1 ratio of soybean oil:DC 193 surfactant obtained from Dow-Corning) was utilized. The solution was prepared by blending oil, water, and surfactant using a blender at high rpm for 3 min. Fouling experiments were performed using the dead-end filtration equipment described above. First, deionized water was filtered through the membrane until the flux stabilized at 7.8 L m<sup>-2</sup> h<sup>-1</sup> for all membranes. The cell and reservoir were filled with the prepared oil-in-water emulsion. Membranes were exposed to the fouling solution for 25 h. Membranes were gently rinsed with DI water before measuring the final flux. As a control, we performed the same fouling test on a commercial membrane with similar pore size, NP030, a poly(ether sulfone) (PES) membrane (Sterlitech).

ASSOCIATED CONTENT

**Supporting Information** 

Materials, copolymer synthesis, <sup>1</sup>H NMR spectra of copolymers, ATR-FTIR spectra of

copolymers, modulated DSC curves, water contact angles, hydrodynamic and calculated diameters

of solutes, solutes rejections, and details of fouling experiments.

**AUTHOR INFORMATION** 

**Corresponding Author** 

Ayse Asatekin - Department of Chemical and Biological Engineering, Tufts University, Medford,

Massachusetts 02155, United States; orcid.org/0000-0002-4704-1542;

Email: ayse.asatekin@tufts.edu

**Funding Sources** 

This research was supported by the National Science Foundation (NSF) under grant nos. CBET-

1553661, DMR-2003629, and NIH grant 1R21GM141683-01.

**Notes** 

The authors declare the following competing financial interest(s): Ayse Asatekin owns a minor

equity in and serves as the Senior Scientific Advisor of ZwitterCo. Inc., which holds a license from

Tufts University to commercialize the technology described in this manuscript. Samuel Lounder

is currently an employee of ZwitterCo; however, his work on this project was performed while he

was a Tufts University student before joining the company. Luca Mazzaferro declares no conflict

of interest.

30

### **ACKNOWLEDGEMENTS**

We gratefully acknowledge financial support from the National Science Foundation (NSF) under grant nos. CBET-1553661 and DMR-2003629. We thank Dr. Nicki Watson at the Harvard Center for Nanoscale Systems (CNS), for collecting TEM images, Prof. Peggy Cebe for access to thermal analysis facilities, and Prof. Qiaobing Xu for access to DLS. We thank the Center for Nanoscale Systems (CNS), where FESEM images were collected, a member of the National Nanotechnology Coordinated Infrastructure Network (NNCI), was supported by the National Science Foundation under NSF award no. 1541959. We thank Solecta membranes for donating PS35 support membranes.

#### REFERENCES

- 1. Sholl, D. S.; Lively, R. P. Seven Chemical Separations to Change the World. *Nature* **2016**, 532 (7600), 435-437.
- 2. He, X.; Hagg, M. B. Membranes for Environmentally Friendly Energy Processes. *Membranes (Basel)* **2012**, *2* (4), 706-26.
- 3. Mauter, M. S.; Zucker, I.; Perreault, F.; Werber, J. R.; Kim, J. H.; Elimelech, M. The Role of Nanotechnology in Tackling Global Water Challenges. *Nat. Sustain.* **2018**, *I* (4), 166-175.
- 4. Mohammad, A. W.; Teow, Y. H.; Ang, W. L.; Chung, Y. T.; Oatley-Radcliffe, D. L.; Hilal, N. Nanofiltration Membranes Review: Recent Advances and Future Prospects. *Desalination* **2015**, *356*, 226-254.
- 5. Van der Bruggen, B.; Vandecasteele, C. Removal of Pollutants from Surface Water and Groundwater by Nanofiltration: Overview of Possible Applications in the Drinking Water Industry. *Environ. Pollut.* **2003**, *122* (3), 435-445.
- 6. Bader, M. S. H. Sulfate Removal Technologies for Oil Fields Seawater Injection Operations. *J. Pet. Sci. Eng.* **2007**, *55* (1-2), 93-110.
- 7. Greenlee, L. F.; Lawler, D. F.; Freeman, B. D.; Marrot, B.; Moulin, P. Reverse Osmosis Desalination: Water Sources, Technology, and Today's Challenges. *Water Res.* **2009**, *43* (9), 2317-2348.
- 8. Jafari, M.; Vanoppen, M.; van Agtmaal, J. M. C.; Cornelissen, E. R.; Vrouwenvelder, J. S.; Verliefde, A.; van Loosdrecht, M. C. M.; Picioreanu, C. Cost of Fouling in Full-Scale Reverse Osmosis and Nanofiltration Installations in the Netherlands. *Desalination* **2021**, *500*, 114865.

- 9. Sadmani, A. H. M. A.; Andrews, R. C.; Bagley, D. M. Nanofiltration of Pharmaceutically Active and Endocrine Disrupting Compounds as a Function of Compound Interactions with Dom Fractions and Cations in Natural Water. *Sep. Purif. Technol.* **2014**, *122*, 462-471.
- 10. Azais, A.; Mendret, J.; Gassara, S.; Petit, E.; Deratani, A.; Brosillon, S. Nanofiltration for Wastewater Reuse: Counteractive Effects of Fouling and Matrice on the Rejection of Pharmaceutical Active Compounds. *Sep. Purif. Technol.* **2014**, *133*, 313-327.
- 11. Martins, A. C.; Oshiro, M. Y.; Albericio, F.; De la Torre, B. G.; Pereira, G. J. V.; Gonzaga, R. V. Trends and Perspectives of Biological Drug Approvals by the Fda: A Review from 2015 to 2021. *Biomedicines* **2022**, *10* (9), 2325.
- 12. Matsuda, Y. Current Approaches for the Purification of Antibody-Drug Conjugates. *J. Sep. Sci.* **2022**, *45* (1), 27-37.
- 13. Hong, S. U.; Bruening, M. L. Separation of Amino Acid Mixtures Using Multilayer Polyelectrolyte Nanofiltration Membranes. *J. Membr. Sci.* **2006**, *280* (1-2), 1-5.
- 14. Ku, J. R.; Lai, S. M.; Ileri, N.; Ramirez, P.; Mafe, S.; Stroeve, P. Ph and Ionic Strength Effects on Amino Acid Transport through Au-Nanotubule Membranes Charged with Self-Assembled Monolayers. *J. Phys. Chem. C* **2007**, *111* (7), 2965-2973.
- 15. Shim, Y. K.; Chellam, S. Steric and Electrostatic Interactions Govern Nanofiltration of Amino Acids. *Biotechnol. Bioeng.* **2007**, *98* (2), 451-461.
- 16. Wang, K. Y.; Chung, T. S. The Characterization of Flat Composite Nanofiltration Membranes and Their Applications in the Separation of Cephalexin. *J. Membr. Sci.* **2005**, *247* (1-2), 37-50.

- 17. Wang, K. Y.; Xiao, Y. C.; Chung, T. S. Chemically Modified Polybenzimidazole Nanofiltration Membrane for the Separation of Electrolytes and Cephalexin. *Chem. Eng. Sci.* **2006**, *61* (17), 5807-5817.
- 18. Nishizawa, M.; Menon, V. P.; Martin, C. R. Metal Nanotubule Membranes with Electrochemically Switchable Ion-Transport Selectivity. *Science* **1995**, *268* (5211), 700-2.
- 19. Nunes, S. P. Block Copolymer Membranes for Aqueous Solution Applications. *Macromolecules* **2016**, *49* (8), 2905-2916.
- 20. Sadeghi, I.; Kaner, P.; Asatekin, A. Controlling and Expanding the Selectivity of Filtration Membranes. *Chem. Mater.* **2018**, *30* (21), 7328-7354.
- 21. Baker, R. W. Research Needs in the Membrane Separation Industry: Looking Back, Looking Forward. *J. Membr. Sci.* **2010**, *362* (1-2), 134-136.
- 22. Bengani, P.; Kou, Y. M.; Asatekin, A. Zwitterionic Copolymer Self-Assembly for Fouling Resistant, High Flux Membranes with Size-Based Small Molecule Selectivity. *J. Membr. Sci.* **2015**, *493*, 755-765.
- 23. Bengani-Lutz, P.; Converse, E.; Cebe, P.; Asatekin, A. Self-Assembling Zwitterionic Copolymers as Membrane Selective Layers with Excellent Fouling Resistance: Effect of Zwitterion Chemistry. *ACS Appl. Mater. Interfaces* **2017**, *9* (24), 20859-20872.
- 24. Rezakazemi, M.; Dashti, A.; Harami, H. R.; Hajilari, N.; Inamuddin Fouling-Resistant Membranes for Water Reuse. *Environ. Chem. Lett.* **2018**, *16* (3), 715-763.
- 25. Weinman, S. T.; Bass, M.; Pandit, S.; Herzberg, M.; Freger, V.; Husson, S. M. A Switchable Zwitterionic Membrane Surface Chemistry for Biofouling Control. *J. Membr. Sci.* **2018**, *548*, 490-501.

- 26. Asatekin, A.; Vannucci, C. Self-Assembled Polymer Nanostructures for Liquid Filtration Membranes: A Review. *Nanosci. Nanotech. Let.* **2015,** *7* (1), 21-32.
- 27. Kaner, P.; Bengani-Lutz, P.; Sadeghi, I.; Asatekin, A. Responsive Filtration Membranes by Polymer Self-Assembly. *Technology* **2016**, *4* (4), 217-228.
- 28. Esfahani, M. R.; Aktij, S. A.; Dabaghian, Z.; Firouzjaei, M. D.; Rahimpour, A.; Eke, J.; Escobar, I. C.; Abolhassani, M.; Greenlee, L. F.; Esfahani, A. R.; Sadmani, A.; Koutahzadeh, N. Nanocomposite Membranes for Water Separation and Purification: Fabrication, Modification, and Applications. *Sep. Purif. Technol.* **2019**, *213*, 465-499.
- 29. Sadeghi, I.; Asatekin, A. Membranes with Functionalized Nanopores for Aromaticity-Based Separation of Small Molecules. *ACS Appl. Mater. Interfaces* **2019**, *11* (13), 12854-12862.
- 30. Sadeghi, I.; Kronenberg, J.; Asatekin, A. Selective Transport through Membranes with Charged Nanochannels Formed by Scalable Self-Assembly of Random Copolymer Micelles. *ACS Nano* **2018**, *12* (1), 95-108.
- 31. Bengani-Lutz, P.; Sadeghi, I.; Lounder, S. J.; Panzer, M. J.; Asatekin, A. High Flux Membranes with Ultrathin Zwitterionic Copolymer Selective Layers with Similar to 1 Nm Pores Using an Ionic Liquid Cosolvent. *ACS Appl. Polym. Mater.* **2019**, *I* (8), 1954-1959.
- 32. Hoffman, J. R.; Phillip, W. A. Dual-Functional Nanofiltration Membranes Exhibit Multifaceted Ion Rejection and Antifouling Performance. *ACS Appl. Mater. Interfaces* **2020**, *12* (17), 19944-19954.
- 33. Park, C.; Yoon, J.; Thomas, E. L. Enabling Nanotechnology with Self Assembled Block Copolymer Patterns. *Polymer* **2003**, *44* (22), 6725-6760.
- 34. Mai, Y.; Eisenberg, A. Self-Assembly of Block Copolymers. *Chem. Soc. Rev.* **2012**, *41* (18), 5969-85.

- 35. Li, L.; Raghupathi, K.; Song, C.; Prasad, P.; Thayumanavan, S. Self-Assembly of Random Copolymers. *Chem. Commun.* **2014**, *50* (88), 13417-32.
- 36. Lounder, S. J.; Asatekin, A. Biomimetic Interaction-Based Ion Selectivity Exhibited by Self-Assembled, Cross-Linked Zwitterionic Copolymer Membranes. *Proc. Natl. Acad. Sci. U.S.A.* **2021,** *118* (37), e2022198118.
- 37. Lounder, S. J.; Asatekin, A. Zwitterionic Ion-Selective Membranes with Tunable Subnanometer Pores and Excellent Fouling Resistance. *Chem. Mater.* **2021**, *33* (12), 4408-4416.
- 38. Ladd, J.; Zhang, Z.; Chen, S.; Hower, J. C.; Jiang, S. Zwitterionic Polymers Exhibiting High Resistance to Nonspecific Protein Adsorption from Human Serum and Plasma. *Biomacromolecules* **2008**, *9* (5), 1357-61.
- 39. Bernards, M.; He, Y. Polyampholyte Polymers as a Versatile Zwitterionic Biomaterial Platform. *J. Biomater. Sci. Polym. Ed.* **2014,** *25* (14-15), 1479-1488.
- 40. Dobbins, S. C.; McGrath, D. E.; Bernards, M. T. Nonfouling Hydrogels Formed from Charged Monomer Subunits. *J. Phys. Chem. B* **2012**, *116* (49), 14346-52.
- 41. Straub, A. P.; Asa, E.; Zhang, W.; Nguyen, T. H.; Herzberg, M. In-Situ Graft-Polymerization Modification of Commercial Ultrafiltration Membranes for Long-Term Fouling Resistance in a Pilot-Scale Membrane Bioreactor. *Chem. Eng. J.* **2020**, *382*, 122865.
- 42. Zhang, W.; Yang, Z.; Kaufman, Y.; Bernstein, R. Surface and Anti-Fouling Properties of a Polyampholyte Hydrogel Grafted onto a Polyethersulfone Membrane. *J. Colloid Interface Sci.* **2018**, *517*, 155-165.
- 43. Kudaibergenov, S.; Koetz, J.; Nuraje, N. Nanostructured Hydrophobic Polyampholytes: Self-Assembly, Stimuli-Sensitivity, and Application. *Adv. Compos. Hybrid Mater.* **2018,** *I* (4), 649-684.

- 44. Zurick, K. M.; Bernards, M. Recent Biomedical Advances with Polyampholyte Polymers. *J. Appl. Polym. Sci.* **2014**, *131* (6), 40069.
- 45. Geise, G. M.; Paul, D. R.; Freeman, B. D. Fundamental Water and Salt Transport Properties of Polymeric Materials. *Prog. Polym. Sci.* **2014**, *39* (1), 1-42.
- 46. Li, X. J.; Zhou, Z. H.; Zhao, Y. Z.; Ramella, D.; Luan, Y. Copper-Doped Sulfonic Acid-Functionalized Mil-101(Cr) Metal-Organic Framework for Efficient Aerobic Oxidation Reactions. *Appl. Organomet. Chem.* **2020**, *34* (4), e5445.
- 47. Jung, H.-Y.; Kim, J. W. Role of the Glass Transition Temperature of Nafion 117 Membrane in the Preparation of the Membrane Electrode Assembly in a Direct Methanol Fuel Cell (Dmfc). *Int. J. Hydrogen Energy* **2012**, *37* (17), 12580-12585.
- 48. Christie, D.; Register, R. A.; Priestley, R. D. Direct Measurement of the Local Glass Transition in Self-Assembled Copolymers with Nanometer Resolution. *ACS Cent. Sci.* **2018**, *4* (4), 504-511.
- 49. Govinna, N.; Sadeghi, I.; Asatekin, A.; Cebe, P. Thermal Properties and Structure of Electrospun Blends of Pvdf with a Fluorinated Copolymer. *J. Polym. Sci., Part B: Polym. Phys.* **2019,** *57* (6), 312-322.
- 50. Deng, G. D.; Schoch, T. D.; Cavicchi, K. A. Systematic Modification of the Glass Transition Temperature of Ion-Pair Comonomer Based Polyelectrolytes and Ionomers by Copolymerization with a Chemically Similar Cationic Monomer. *Gels* **2021**, *7* (2), 45.
- 51. Asatekin, A.; Olivetti, E. A.; Mayes, A. M. Fouling Resistant, High Flux Nanofiltration Membranes from Polyacrylonitrile-Graft-Poly(Ethylene Oxide). *J. Membr. Sci.* **2009**, *332* (1-2), 6-12.

- 52. Zydney, A., Charged Ultrafiltration Membrane. In *Encyclopedia of Membranes*, Drioli, E.; Giorno, L., Eds. Springer Berlin Heidelberg: Berlin, Heidelberg, 2015; pp 1-2.
- 53. Singh, S.; Khulbe, K. C.; Matsuura, T.; Ramamurthy, P. Membrane Characterization by Solute Transport and Atomic Force Microscopy. *J. Membr. Sci.* **1998**, *142* (1), 111-127.
- 54. Bowen, W. R.; Mohammad, A. W. Diafiltration by Nanofiltration: Prediction and Optimization. *AlChE J.* **1998**, *44* (8), 1799-1812.
- 55. Nisato, G.; Munch, J. P.; Candau, S. J. Swelling, Structure, and Elasticity of Polyampholyte Hydrogels. *Langmuir* **1999**, *15* (12), 4236-4244.
- 56. Blackman, L. D.; Gunatillake, P. A.; Cass, P.; Locock, K. E. S. An Introduction to Zwitterionic Polymer Behavior and Applications in Solution and at Surfaces. *Chem. Soc. Rev.* **2019**, *48* (3), 757-770.
- 57. Higgs, P. G.; Joanny, J. F. Theory of Polyampholyte Solutions. *J. Chem. Phys.* **1991,** *94* (2), 1543-1554.
- 58. Nair, K. S.; Manu, B.; Azhoni, A. Sustainable Treatment of Paint Industry Wastewater: Current Techniques and Challenges. *J. Environ. Manage.* **2021**, *296*, 113105.
- 59. Roy, Y.; Warsinger, D. M.; Lienhard, V. J. H. Effect of Temperature on Ion Transport in Nanofiltration Membranes: Diffusion, Convection and Electromigration. *Desalination* **2017**, *420*, 241-257.
- 60. Carter, B. M.; Wiesenauer, B. R.; Noble, R. D.; Gin, D. L. Thin-Film Composite Bicontinuous Cubic Lyotropic Liquid Crystal Polymer Membranes: Effects of Anion-Exchange on Water Filtration Performance. *J. Membr. Sci.* **2014**, *455*, 143-151.

- 61. Epsztein, R.; Shaulsky, E.; Dizge, N.; Warsinger, D. M.; Elimelech, M. Role of Ionic Charge Density in Donnan Exclusion of Monovalent Anions by Nanofiltration. *Environ. Sci. Technol.* **2018**, *52* (7), 4108-4116.
- 62. Hurwitz, G.; Bhattacharjee, S.; Seo, E.; Wang, J.; Severt, A.; Temple, J.; Nguyen, J.; Koehler, J.; Hoek, E. M. V. Field Testing of Polycera (R), Pes, and Pvdf Ultrafiltration Membranes in Municipal Tertiary Filtration: Impacts of Membrane Polymer Chemistry on Fouling, Cleaning, Energy, and Cost. *Desalin. Water Treat.* **2018**, *111*, 39-47.
- 63. Barcellona, M. N.; Johnson, N.; Bernards, M. T. Characterizing Drug Release from Nonfouling Polyampholyte Hydrogels. *Langmuir* **2015**, *31* (49), 13402-9.
- 64. Herzberg, M.; Sweity, A.; Brami, M.; Kaufman, Y.; Freger, V.; Oron, G.; Belfer, S.; Kasher, R. Surface Properties and Reduced Biofouling of Graft-Copolymers That Possess Oppositely Charged Groups. *Biomacromolecules* **2011**, *12* (4), 1169-1177.
- 65. Madaeni, S. S.; Gheshlaghi, A.; Rekabdar, F. Membrane Treatment of Oily Wastewater from Refinery Processes. *Asia-Pac. J. Chem. Eng.* **2013**, *8* (1), 45-53.
- 66. Wandera, D.; Wickramasinghe, S. R.; Husson, S. M. Modification and Characterization of Ultrafiltration Membranes for Treatment of Produced Water. *J. Membr. Sci.* **2011**, *373* (1-2), 178-188.
- 67. Kaner, P.; Rubakh, E.; Kim, D. H.; Asatekin, A. Zwitterion-Containing Polymer Additives for Fouling Resistant Ultrafiltration Membranes. *J. Membr. Sci.* **2017**, *533*, 141-159.
- 68. Asatekin, A.; Mayes, A. M. Oil Industry Wastewater Treatment with Fouling Resistant Membranes Containing Amphiphilic Comb Copolymers. *Environ. Sci. Technol.* **2009**, *43* (12), 4487-4492.

- 69. Bengani-Lutz, P.; Zaf, R. D.; Culfaz-Emecen, P. Z.; Asatekin, A. Extremely Fouling Resistant Zwitterionic Copolymer Membranes with Similar to 1 Nm Pore Size for Treating Municipal, Oily and Textile Wastewater Streams. *J. Membr. Sci.* **2017**, *543*, 184-194.
- 70. Venugopal, V. Valorization of Seafood Processing Discards: Bioconversion and Bio-Refinery Approaches. *Front. Sustain. Food Syst.* **2021**, *5*, 611835.

# For Table of Contents Only:

